

# 中国激光

## 环烯烃共聚物表面减反膜的制备及其可靠性研究

付秀华<sup>1</sup>, 李俊纬<sup>1\*</sup>, 张功<sup>1</sup>, 张静<sup>1</sup>, 金海俊<sup>2</sup>, 李爽<sup>2</sup>

<sup>1</sup> 长春理工大学光电工程学院, 吉林 长春 130022;

<sup>2</sup> 光驰科技(上海)有限公司, 上海 200444

**摘要** 高分子材料以其优异的性能, 近年来得到了广泛的应用。以一种新型高分子材料环烯烃共聚物为基底, 设计并研制了 400~700 nm 波段的减反射膜。根据薄膜热应力理论分析了材料特性, 选择 ZrO<sub>2</sub> 作为黏结层, 研究了等离子体处理时间对基底表面微观结构以及化学组成的影响。通过优化工艺参数和增加基底表面的活性, 提高了基底与黏结层的结合力, 再通过过渡层将黏结层与镀层结合, 解决了薄膜与基底热膨胀系数不匹配的问题。采用镀后离子束轰击技术解决了恒温恒湿时的膜裂问题。测试结果表明, 减反射膜在 400~700 nm 波段的平均反射率为 0.117%, 且具备良好的耐环境性能。

**关键词** 薄膜; 光学薄膜; 环烯烃共聚物; 热应力; 等离子体处理; 离子束轰击

中图分类号 O484

文献标志码 A

doi: 10.3788/CJL202148.2403003

### 1 引言

环烯烃共聚物(Cyclic Olefin Copolymer, COC)是一种近年来逐渐引起人们高度重视的无定形高分子材料, 具有覆盖全谱的高光透射率、低双折射系数、极低的吸水率、低密度、不易碎以及高阿贝数、稳定的化学性能、耐酸碱性和优良的力学性能等优点<sup>[1-3]</sup>。与聚甲基丙烯酸甲酯(PMMA)和聚碳酸酯(PC)等传统的透明塑料相比, COC 不仅具有与 PMMA 相当的光学性能, 还具有更高的耐温性。即使在较高的温度下, COC 仍然具有极低的水汽吸收率和良好的抗蠕变性能, 能够更好地保持光学器件的原始设计尺寸。这些正是光学元件所需的优良特性, 因此 COC 被认为是 PC、PMMA 等的理想替代材料, 在光学领域中具有良好的发展前景。

COC 与传统高分子材料类似, 其热膨胀系数较高, 所以会在成膜过程中或成膜后由于温度的变化而发生膜裂或脱膜现象<sup>[4-7]</sup>。国内外针对于 PC 和 PMMA 表面沉积光学薄膜的研究较多, 但是以 COC 为基底的研究却鲜见报道。本文主要针对 400~700 nm 波段设计研制了减反射膜, 对提高 COC 表面光学薄膜的附着力与耐环境适应性能展

开了研究。

### 2 薄膜材料的应力分析及膜系结构设计

#### 2.1 薄膜材料的应力分析

本文使用的基底是日本瑞翁公司生产的 ZEONEX-350R, 其折射率约为 1.509, 具体的物理性质如表 1 所示。

表 1 ZEONEX-350R 的物理性质

Table 1 Physical properties of ZEONEX-350R

Parameter	Value
Refractive index@550 nm	1.509
Water absorption /%	<0.010
Young's modulus / MPa	2800
Glass transition temperature / °C	123
Coefficient of thermal expansion / K <sup>-1</sup>	7.0×10 <sup>-5</sup>
Transmittance /%	92

COC 的热膨胀系数较大, 在成膜过程中或成膜之后会因为外界温度的变化而产生极大的热应力, 膜层容易破裂, 甚至发生整体或局部脱膜现象。因此, 在镀膜前可以将匹配良好、热应力松弛的材料作为黏结层, 并通过过渡层将黏结层与镀层结合<sup>[8]</sup>。

收稿日期: 2021-04-12; 修回日期: 2021-05-07; 录用日期: 2021-05-24

通信作者: \*lijwfilm@126.com

该方法可以大大降低材料失配引起的热应力,防止薄膜中的裂纹沿层间扩展,从而增强薄膜的附着力。

根据所查资料<sup>[9]</sup>,可以计算出第  $i$  层薄膜产生的热应力为

$$\sigma_i = E_i \left( c + \frac{y - t_b}{r} - \alpha_i \Delta T \right), \quad i = 1, 2, 3, \dots, n, \quad (1)$$

$$c = -\frac{\left( E_s t_s \alpha_s + \sum_{i=1}^n E_i t_i \alpha_i \right) \Delta T}{E_s t_s + \sum_{i=1}^n E_i t_i}, \quad (2)$$

$$t_b = \frac{-E_s t_s^2 + \sum_{i=1}^n E_i t_i (2h_{i-1} + t_i)}{2(E_s t_s + \sum_{i=1}^n E_i t_i)}, \quad (3)$$

$$\frac{1}{r} = \frac{3 \left[ E_s (c - \alpha_s \Delta T) t_s^2 - \sum_{i=1}^n E_i t_i (c - \alpha_i \Delta T) (2h_{i-1} + t_i) \right]}{E_s t_s^2 (2t_s + 3t_b) + \sum_{i=1}^n E_i t_i [6h_{i-1} t_i + 2t_i^2 - 3t_b (2h_{i-1} + t_i)]}, \quad (4)$$

式中: $\sigma_i$  为第  $i$  层薄膜所产生的热应力; $y$  为膜层总厚度; $\Delta T$  为温度变化量; $n$  为膜层总层数; $E_i$ 、 $t_i$  和  $\alpha_i$  分别为第  $i$  层薄膜的杨氏模量、厚度和热膨胀系数; $E_s = 2800$  MPa 为基底的杨氏模量; $t_s = 5$  mm 为基底的厚度; $\alpha_s = 7.0 \times 10^{-5}$  K<sup>-1</sup> 为基底的热膨胀

系数; $h_i$  为前  $i$  层薄膜的总厚度。由于薄膜制备时不加热,因此假设沉积过程中温度为 50 °C,环境温度选取 20 °C,即温度变化量  $\Delta T = 30$  °C。当  $i = 1$  时,假定第一层薄膜厚度为 30 nm,计算出几种常用可见光波段薄膜材料的热应力参数,结果如表 2 所示。

表 2 薄膜的热学与力学参数  
Table 2 Thermal and mechanical parameters of thin films

Material	Coefficient of thermal expansion /( $10^{-6}$ K <sup>-1</sup> )	Young's modulus /GPa	Thermal stress /( $10^8$ Pa)
Ta <sub>2</sub> O <sub>5</sub>	6.6	115	4.221
H4	9.2	220	4.079
Ti <sub>3</sub> O <sub>5</sub>	8.8	230	4.292
ZrO <sub>2</sub>	12.8	113	1.938
SiO <sub>2</sub>	0.8	170	12.619
MgF <sub>2</sub>	8.9	138.5	3.897
Al <sub>2</sub> O <sub>3</sub>	5.0	230	4.413

根据表 2 可以看出,当 ZrO<sub>2</sub> 作为第一层薄膜材料时,热应力最小,因此采用 ZrO<sub>2</sub> 作为黏结层材料。

可见光范围内常用的高折射率材料有 Ti<sub>3</sub>O<sub>5</sub>、H4(钛酸镧 La<sub>2</sub>Ti<sub>2</sub>O<sub>7</sub>)和 Ta<sub>2</sub>O<sub>5</sub>。考虑到材料折射率、材料热膨胀系数与基底热膨胀系数的匹配以及低温下成膜的稳定性,最终选取 Ti<sub>3</sub>O<sub>5</sub> 作为高折射率材料。

可见光范围内常用的低折射率材料有 MgF<sub>2</sub>、SiO<sub>2</sub> 和 L5,其中 L5 是 SiO<sub>2</sub> 与 Al<sub>2</sub>O<sub>3</sub> 的混合物。

SiO<sub>2</sub> 薄膜具有稳定的性能和较强的力学性能,与 Ti<sub>3</sub>O<sub>5</sub> 复合后能有效降低薄膜的内应力;而电子束蒸发沉积的 Al<sub>2</sub>O<sub>3</sub> 薄膜结构较为致密,没有大的柱状孔隙,能防止空气中的水分渗入到薄膜结构中,在与 SiO<sub>2</sub> 结合后,颗粒之间生成稳定致密的氧桥键 Si—O—Al,能够限制 SiO<sub>2</sub> 的水解作用<sup>[10]</sup>。因此,考虑到材料的稳定性以及后面的环境测试要求,最终选取 L5 作为低折射率材料。

## 2.2 膜系结构设计

基于光学薄膜的设计理论,采用双有效界面法

设计可见光波段减反射膜的膜系。使用 Macleod 膜系设计软件中的共轭梯度(Conjugate Gradient)法和单纯形(Simplex)优化方法对初始膜系进行优化,优化后的膜系结构为 Sub|0.037M 0.027H 0.072L 0.46H 0.088L 0.093H 0.094L 0.43H 0.21L|Air,其中 Sub 代表 ZEONEX-350R, M 代表  $\text{ZrO}_2$ , H 代表  $\text{Ti}_3\text{O}_5$ , L 代表 L5, Air 代表空气,设计的单面减反射膜的理论平均反射率为 0.093%,曲线如图 1 所示。

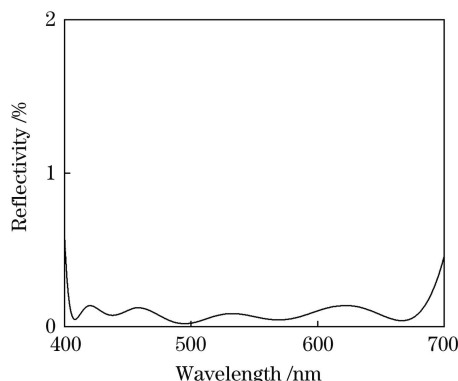


图 1 理论设计曲线  
Fig. 1 Theoretical design curve

### 3 薄膜制备技术的研究

#### 3.1 膜-基脱落机理分析

本实验在光驰 OTFC-1800X 型真空镀膜机上完成。在镀膜之前,需对基底进行清洁和退火处理,避免划痕、残留水汽与灰尘以及注塑成型时的内应力导致沉积的薄膜不牢固<sup>[11]</sup>。将预处理后的基底放置在真空室内,待真空中度达到  $5 \times 10^{-4}$  Pa 时开始沉积薄膜。因为 COC 基底的热膨胀系数比较大,所以沉积选择在室温下进行。但室温下成膜会出现薄膜聚集密度降低的现象,所以在不使真空中度过高的前提下,采用离子束辅助沉积来提高沉积粒子的迁移率和膜层的填充密度。由于基板玻璃的转化温度为 123 ℃,为了使基板的热应力尽量小,实际镀膜基板的温度应尽可能低并有一定可调空间。测试了离子源参数对基板温度的影响,工艺参数如表 3 所示,其中 DOE 表示实验设计,Beam 为离子源放出的辉光,其能量大小与离子源电流和电压呈正相关,ACC 为离子源加速极的电压, $E/B$  为中和器与 Beam 电流之比,离子源(IBS)可通入氧气与氩气,中和器仅通入氩气。

表 3 离子源辅助沉积工艺参数

Table 3 Process parameters for ion beam source assisted deposition

DOE No.	Beam		ACC / V	$E/B$ / %	Flow rate of O <sub>2</sub> in IBS / (mL·min <sup>-1</sup> )	Flow rate of Ar in IBS / (mL·min <sup>-1</sup> )	Flow rate of Ar in neutralizer / (mL·min <sup>-1</sup> )	Temperature / ℃
	Voltage / V	Current / mA						
1								65
2	300	300	350	150	50	0	8	79
3	350	350	400	150	50	0	8	87
4	400	400	450	150	50	0	8	94
5	500	500	550	150	50	0	8	104

对 5 组实验后的样片分别进行拉膜测试,结果均脱膜严重,但 DOE 3 相对较好,其脱膜显微照片如图 2 所示,且成膜后基板温度相对较低,所以最终选取 DOE 3 的条件研究其他因素对膜层结合力的影响。



图 2 脱膜样片显微照片  
Fig. 2 Micrograph of sample film detachment

COC 基底的单体结构如图 3 所示,其无活性官能团,所以表面活性较低。因此,在 COC 与薄膜材料结合时,界面两侧的原子只是简单的机械和物理结合,不能够形成强化学键合,这会导致薄膜的附着力非常低。可以将基底表面的单体氧化以生成 -OH,增加氧元素含量,提高活性,从而使薄膜材料与基底之间形成化学键合以提高薄膜的附着力。

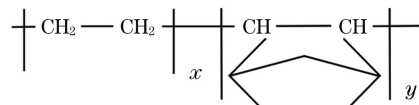


图 3 COC 单体结构分子式  
Fig. 3 Structural formula of COC monomer

### 3.2 表面等离子体处理技术研究

等离子体处理是利用等离子体中的电子、离子等高能粒子在基底表面的氧化反应和刻蚀作用,增加基底表面的极性和粗糙度,进而增强基底与薄膜之间的化学键合和物理嵌合性。等离子体处理只作

用于基底表面的薄层,仅改变几十到几百纳米厚度层的理化性质,并不会对本体的力学性能造成影响<sup>[12]</sup>,所以为了增加基底表面的活性,分别在不同的等离子体处理时间下进行了测试研究,具体工艺参数如表4所示。

表4 等离子体处理工艺参数

Table 4 Technological parameters for plasma treatment

Time / min	Beam		ACC / V	$E/B$ / %	Flow rate of O <sub>2</sub> in IBS / (mL·min <sup>-1</sup> )	Flow rate of Ar in IBS / (mL·min <sup>-1</sup> )	Flow rate of Ar in neutralizer / (mL·min <sup>-1</sup> )
	Voltage / V	Current / mA					
5	500	500	600	150	90	5	8
10	500	500	600	150	90	5	8
15	500	500	600	150	90	5	8

对测试后的基底表面进行X射线光电子能谱(XPS)测试,以确定表面化学元素及官能团含量随等离子处理时间的变化规律,其结果如图4所示。

利用图4计算得出了基底表面的氧元素相对含量(原子数分数)随等离子体处理时间的变化曲线,如图5所示。可以看出,在经过等离子体处理后,基底表面的氧元素含量都有不同程度的增加,但基底表面的氧元素相对含量与等离子体处理时间并不是

呈简单的线性关系。经过分析,当处理时间为5 min时,作用于基底表面的活性粒子较少,只有少量的基团参与反应;当处理时间为10 min时,表面的氧元素含量达到最大;而当处理时间为15 min时,基底表面参与反应的基团已经达到饱和,过长时期的等离子体处理使得原本引入的氧元素以及新形成的官能团被高能粒子破坏掉,所以最终等离子体处理时间选为10 min。

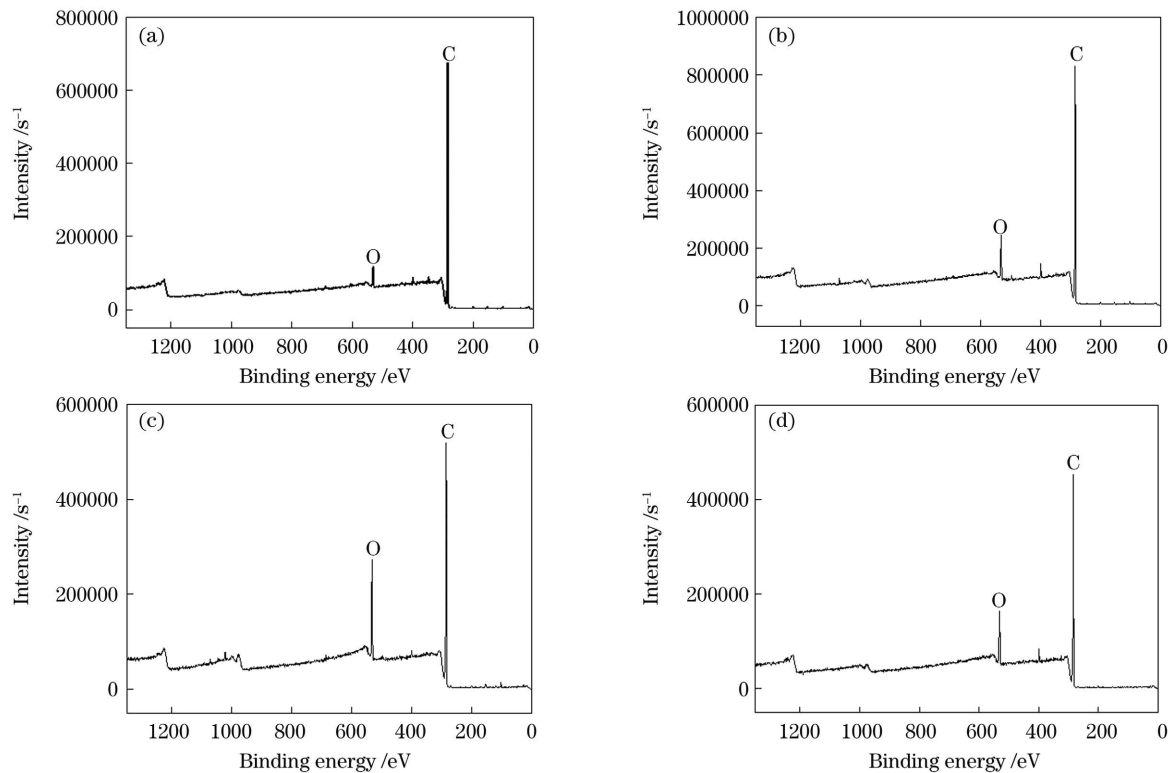


图4 不同样等离子体处理时间下基底表面的XPS测试结果。(a)未处理;(b)5 min;(c)10 min;(d)15 min

Fig. 4 XPS test results of substrate surface after plasma treatment with different time. (a) Untreated; (b) 5 min; (c) 10 min; (d) 15 min

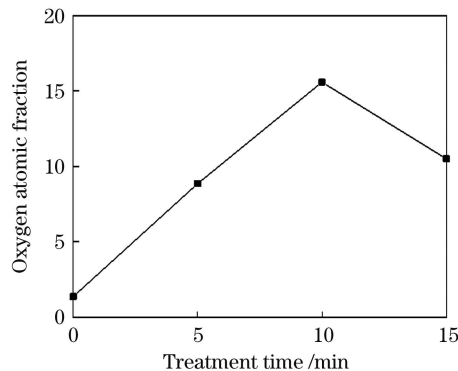


图 5 表面氧元素的原子数分数随处理时间的变化曲线

Fig. 5 Variation of surface oxygen atomic fraction with treatment time

### 3.3 膜-膜结合力研究

利用 3M 胶带粘拉经过等离子体处理后制备的薄膜,仍出现部分脱膜现象。通过观察发现,薄膜并非全部脱落,仍有部分附着在基底上。对样片的脱膜位置进行光谱测试,其结果如图 6 所示。

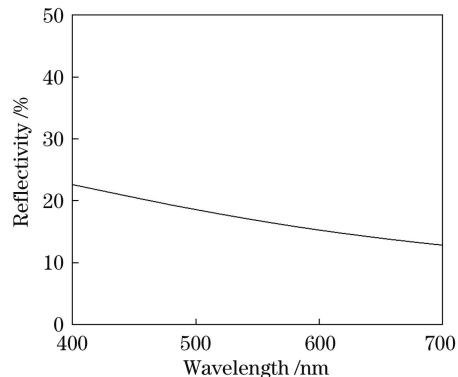


图 6 样片脱膜位置的光谱曲线

Fig. 6 Spectral curve at sample film detachment position

样片脱膜位置的光谱图与单层  $\text{ZrO}_2$  的光谱基本一致,经分析可能是因为膜系中黏结层与基底结合好,但黏结层与镀层之间的附着力较小,所以判断脱膜现象存在于黏结层  $\text{ZrO}_2$  与镀层之间的  $\text{Ti}_3\text{O}_5$  中。在当前工艺条件下,  $\text{ZrO}_2$  和  $\text{Ti}_3\text{O}_5$  膜层同属于张应力性质,文献[13]提出用力矩来判断薄膜是否发生破裂或分层。分析此时力矩,发现膜层会发生分层现象,因此应在两者之间增镀具有压应力性质的过渡层。当选择 L5 作为过渡层材料时,对膜系重新进行优化设计,得到膜系:Sub|0.037M 0.134L 0.072H 0.138L 0.06H 0.349L 0.032H 0.115L 0.457H 0.225L|Air,平均反射率为 0.102%,再次分析此时的力矩,膜层分层受到抑制,制备完成后样片未出现脱膜现象。对两种膜系结构的样片进行电镜扫描(SEM)测试,其横截面如图 7 所示。

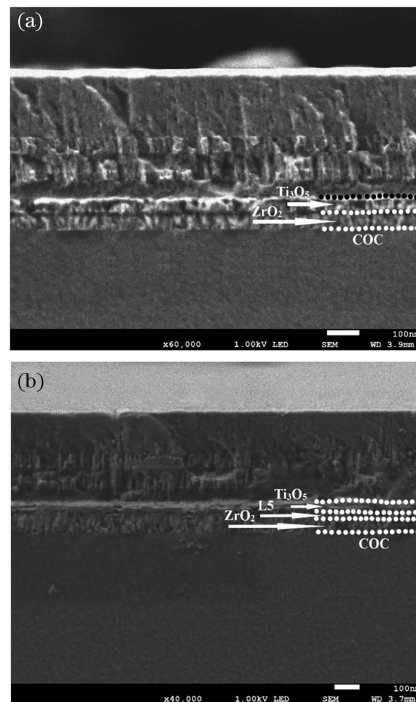


图 7 薄膜横截面图。(a) 增镀 L5 前;(b) 增镀 L5 后

Fig. 7 Cross section images of thin films. (a) Before coating L5; (b) after coating L5

从图 7(a)可以看出,  $\text{ZrO}_2$  与  $\text{Ti}_3\text{O}_5$  之间有明显的分层,说明二者之间的吸附主要是物理吸附,结合力主要为范德瓦耳斯力。如图 7(b)所示,在黏结层与镀层之间增镀一层 L5 后,膜层之间的界限变得不明显,说明膜层之间形成了扩散层,L5 中的 Si—O 键分别与  $\text{ZrO}_2$  和  $\text{Ti}_3\text{O}_5$  结合,形成了 Si—O—Zr 以及 Si—O—Ti 键,化学吸附大大提高了薄膜的牢固度。

## 4 测试结果及工艺优化

### 4.1 光谱性能测试

为了减小测量误差,对样片背面作磨砂效果并涂消光黑漆,之后采用 LRMS-600P1 显微分光测试仪对其光谱特性进行测试,测试结果如图 8 所示。

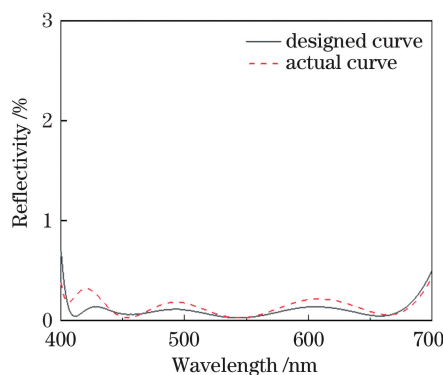


图 8 设计与实际测试光谱对比图

Fig. 8 Comparison of designed and actual test spectra

测试结果与设计曲线的波形基本相同,且该减反射膜在400~700 nm波段的平均反射率为0.117%,相比设计提高了0.015%,符合随机误差的实际效果。

#### 4.2 耐环境性能测试

针对薄膜的耐环境性能,对薄膜进行了一系列的测试,测试结果如表5所示。

表5 环境测试项目及结果

Table 5 Environmental test items and results

Test item	Test method	Experimental phenomenon	Test result
Film adhesion test	3M tape with viscosity of no less than 3 N/cm <sup>2</sup> is used to quickly stretch sample surface film from edge to center in vertical direction of coated surface	No film layer shedding	Passed
High and low temperature test	Without packaging, sample is kept at -40 °C and 85 °C for 24 h	No crack in film layer	Passed
Constant temperature and humidity test	Under condition of no packaging, sample is put into constant temperature and humidity test chamber with temperature of 85 °C and relative humidity of 85% for 24 h	No crack in film layer	Failed

#### 4.3 工艺优化

对样片进行恒温恒湿测试24 h后,薄膜出现了膜裂现象,如图9所示。

从图9中可以看出,膜裂部位呈边缘向中心挤压的形态。这是因为基底的热膨胀系数较大,在成膜过程中虽然采用低能量的离子源进行辅助沉积,但沉积粒子的迁移率较低,膜层不够致密,恒温恒湿测试中的水汽进入到膜层之间,发生膜裂现象。所以为了解决膜裂问题,在薄膜制备后分别采用不同能量的离子源对样片持续轰击5 min以提高膜层的填充密度,工艺参数如表6所示。

对工艺优化后的样片再次进行恒温恒湿测试,

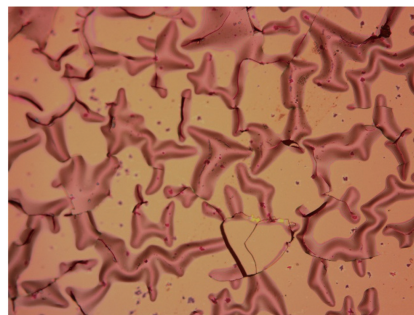


图9 膜裂样片显微照片

Fig. 9 Micrograph of sample film crack

离子源参数为600 V、600 mA时,膜裂现象得到显著改善,如图10所示。

表6 离子源轰击工艺参数

Table 6 Process parameters for ion beam source bombardment

Time / min	Beam		ACC / V	$\frac{E}{B}$ / %	Flow rate of O <sub>2</sub> in IBS / (mL·min <sup>-1</sup> )	Flow rate of Ar in IBS / (mL·min <sup>-1</sup> )	Flow rate of Ar in neutralizer / (mL·min <sup>-1</sup> )
	Voltage / V	Current / mA					
5	400	400	400	150	50	0	8
5	600	600	600	150	50	0	8
5	800	800	800	150	50	0	8



图10 工艺优化后的样片显微照片

Fig. 10 Micrograph of sample after process optimization

最终样片通过了膜层附着力、高低温和恒温恒湿测试。对工艺优化后的样片进行光谱测试,测试曲线与图8基本相同,表明所制备的薄膜具有很好的力学性能以及环境适应性。

## 5 结 论

以环烯烃共聚物为基底,研究了基底与膜料的材料特性。选择ZrO<sub>2</sub>作为黏结层,基底表面经过等离子体处理后,膜-基的结合力得到提高。选择

L5作为过渡层材料,将黏结层与镀层结合,膜层之间在力矩匹配的基础上形成了化学键,提高了膜-膜的结合力。通过镀后离子束轰击技术,解决了膜层不致密在恒温恒湿测试中引起的膜裂问题。最终制备的减反射膜的平均反射率为0.117%,且通过了膜层附着力、高低温和恒温恒湿测试。但是由于成膜过程中的膜层厚度存在随机误差,因此实验结果略高于理论设计。研究薄膜材料的特性,优化薄膜沉积工艺,提高镀膜精度是今后工作的重点研究方向。

## 参考文献

- [1] Guo S Z. Cyclo olefin copolymers—the novel amorphous thermoplastics [J]. Huaxue Shijie (Chemical World), 2001, 42(3): 161-164.  
郭世卓. 环烯烃共聚物:一种新型的非结晶热塑性塑料[J]. 化学世界, 2001, 42(3): 161-164.
- [2] Khanarian G. Optical properties of cyclic olefin copolymers [J]. Optical Engineering, 2001, 40: 1024-1029.
- [3] Yang M Q, Zhang H F, Li L, et al. Synthesis and properties of novel high temperature transparent cyclic olefin copolymers [J]. Journal of Aeronautical Materials, 2017, 37(4): 1-6.  
杨木泉, 张洪峰, 厉蕾, 等. 新型耐高温透明环烯烃共聚物的合成与性能[J]. 航空材料学报, 2017, 37(4): 1-6.
- [4] Fu X H, Liu Y B, Xiong S F, et al. Fabrication of anti-water hard and anti-aging optical film based on plastic lens [J]. Journal of Applied Optics, 2017, 38(1): 0105002.  
付秀华, 刘禹冰, 熊仕富, 等. 基于塑料镜片防水加固抗老化光学薄膜的研制[J]. 应用光学, 2017, 38(1): 0105002.
- [5] Liu D M, Wei B Y, Fu X H, et al. Development of polycarbonate high strength ultra-low reflectivity film [J]. Acta Photonica Sinica, 2020, 49(12): 1231001.  
刘冬梅, 魏博洋, 付秀华, 等. 聚碳酸酯高强度超低反射率薄膜的研制[J]. 光子学报, 2020, 49(12): 1231001.
- [6] Zhang D, Pan Y Q, Liu J Z, et al. Research on ultra-wide band anti-reflection film and its high temperature and humidity resistance of plastics [J]. Optics & Optoelectronic Technology, 2020, 18(4): 106-110.  
张达, 潘永强, 刘金泽, 等. 塑料超宽带减反射膜及抗高温高湿特性研究[J]. 光学与光电技术, 2020, 18(4): 106-110.
- [7] Liu J S, Wang L, Ouyang W, et al. Fabrication of PMMA nanofluidic electrochemical chips with integrated microelectrodes [J]. Biosensors and Bioelectronics, 2015, 72: 288-293.
- [8] Yu F B, Chen Y. The influence factor of thin films adhesion prepared by magnetron sputtering [J]. Insulating Materials, 2008, 41(6): 41-43, 46.  
余凤斌, 陈莹. 磁控溅射对薄膜附着力的影响[J]. 绝缘材料, 2008, 41(6): 41-43, 46.
- [9] Fu X H, Pan Y G, Dong J, et al. The characteristic of connecting layer material on TeO<sub>2</sub> crystal surface by thermal stress method [J]. Acta Photonica Sinica, 2016, 45(1): 0131001.  
付秀华, 潘永刚, 董军, 等. 用热应力法研究二氧化碲晶体表面连接层材料的特性[J]. 光子学报, 2016, 45(1): 0131001.
- [10] Chen M J, Guo Z J, Yin B. Preparation and characterization of scratch-resistant Al<sub>2</sub>O<sub>3</sub>/SiO<sub>2</sub> antireflective film [J]. Acta Energiae Solaris Sinica, 2011, 32(10): 1440-1444.  
陈明洁, 郭志坚, 印冰. Al<sub>2</sub>O<sub>3</sub>/SiO<sub>2</sub> 耐磨增透膜的制备和表征[J]. 太阳能学报, 2011, 32(10): 1440-1444.
- [11] Fu X H, Huang H Y, Zhang J, et al. Anti-reflection protective film of chalcogenide glass substrate and its environmental adaptability [J]. Acta Optica Sinica, 2020, 40(21): 2131002.  
付秀华, 黄宏宇, 张静, 等. 硫系玻璃基底减反保护膜及其耐环境适应性的研究[J]. 光学学报, 2020, 40(21): 2131002.
- [12] Liu Z, Chen B H, Chen P. Treatment of oxygen dielectric barrier discharge plasma on PBO fiber surface and influence on its BMI composites [J]. Chinese Journal of Materials Research, 2020, 34(2): 109-117.  
刘哲, 陈博涵, 陈平. 氧气DBD等离子体处理PBO纤维表面及其对双马树脂基复合材料界面性能的影响[J]. 材料研究学报, 2020, 34(2): 109-117.
- [13] Moore T D, Jarvis J L. The peeling moment: a key rule for delamination resistance in I. C. assemblies [J]. Journal of Electronic Packaging, 2004, 126(1): 106-109.

# Preparation and Reliability of Anti-Reflection Film on Cyclic Olefin Copolymer Surface

Fu Xiuhua<sup>1</sup>, Li Junwei<sup>1\*</sup>, Zhang Gong<sup>1</sup>, Zhang Jing<sup>1</sup>, Jin Haijun<sup>2</sup>, Li Shuang<sup>2</sup>

<sup>1</sup> School of Optoelectronic Engineering, Changchun University of Science and Technology, Changchun, Jilin 130022, China;

<sup>2</sup> Optorun (Shanghai) Co., Ltd., Shanghai 200444, China

## Abstract

**Objective** Cyclic olefin copolymer (COC) is a kind of amorphous polymer material which attracts more and more attention in recent years, and it has many advantages such as high transmittance covering the full spectrum, low birefringence coefficient, very low water absorption, low density, not fragile, high Abbe number, stable chemical properties, acid and alkali resistance, and excellent mechanical properties. Compared with traditional transparent plastics such as polymethyl methacrylate (PMMA) and polycarbonate (PC), COC not only has the same optical performance as PMMA, but also has higher temperature resistance than it. And these characteristics are the excellent properties needed for the preparation of optical elements. Therefore, COC is considered as an ideal substitute material for PC, PMMA, polystyrene, polyvinyl chloride, and some engineering plastics, and has a good development prospect in the optical field. However, COC is similar to traditional polymer materials due to its high coefficient of thermal expansion, and thus film cracking or shedding occurs due to the temperature change during or after film coating. There are many domestic and foreign researches on the deposition of optical films on the surface of PC and PMMA, but there are few reports on the use of COC as the substrate, although COC has good performances in the visible band. Therefore, this paper mainly designs and develops the anti-reflection film for the band of 400–700 nm, and conducts researches on how to improve the adhesion and environmental resistance of optical films on the COC surface.

**Methods** The material characteristics are analyzed according to the thin film thermal stress theory, and the  $\text{ZrO}_2$  with the smallest thermal stress is selected as the adhesive layer by calculating the thermal stress between the first layer material and the substrate. The plasma treatment time of the substrate surface is studied. The XPS test is performed on the surface of the treated sample to find a solution with a relatively high surface oxygen content, and the technological parameters are optimized to solve the problem of film shedding due to the mismatch between the coefficients of thermal expansion of the film and the substrate. It is found that the film layer of the sample after the film pulling test is not completely fell off. Firstly, the shedding position from the spectral curve of the sample is analyzed, and then through the analysis of the moment of film, the transition layer is coated, which improves the adhesion between the coating and the adhesive layer. Finally, the samples with the two structures are tested by SEM. Through the analysis of the micrograph of the film cracking sample after the constant temperature and humidity test, it is found that the film layer is not compact enough, which causes the water vapor to enter the film layer during the test and to change the stress, and the technology of ion beam bombardment after coating is used to increase the film filling density.

**Results and Discussions** The effect of plasma treatment under different time on the content of chemical elements and functional groups on the surface of the substrate is studied (Fig. 4), and the technological parameters are optimized to increase the activity of substrate surface and improve the adhesion between the substrate and the coating. The thermal stresses of different materials with COC as the substrate are analyzed (Table 2), and the  $\text{ZrO}_2$  with the smallest thermal stress is selected as the adhesive layer, which solves the problem of film shedding due to the mismatch between the coefficients of thermal expansion of the film and the substrate. The film layer of the shedding sample is analyzed by the moment of film, and the adhesive layer L5 is coated in the middle, so that the film layers can infiltrate and form chemical bonds on the basis of moment matching (Fig. 7), which greatly improves the adhesion between the film layers. The technology of ion beam bombardment after coating solves the problem of low film aggregation density caused by non-heating in the film formation process (Table 6), and makes the sample pass the constant temperature and humidity test.

**Conclusions** In this paper, the cyclic olefin copolymer is used as the substrate to study the properties of the substrate and the film material. And  $\text{ZrO}_2$  is selected as the adhesive layer and the surface of the substrate is treated with plasma to improve the adhesion between the film and the substrate. Then the moment between the film layers is analyzed and the L5 is selected as the transition layer material to combine the adhesive layer with the coating, so that the film layers can infiltrate and form chemical bonds on the basis of moment matching, which greatly improves the adhesion between the film layers. The technology of ion beam bombardment after coating solves the problem of film cracking in the constant temperature and humidity test due to the non-compact film layer. The test results show that the average reflectivity of the anti-reflection film at 400–700 nm is 0.117%. Furthermore, the anti-reflection film can pass the film adhesion test, the high and low temperature test, and the constant temperature and humidity test, and possesses good environmental adaptability.

**Key words** thin films; optical thin film; cyclic olefin copolymer; thermal stress; plasma treatment; ion beam bombardment

**OCIS codes** 310.1210; 310.1860; 310.3840